PHYSICS AND CHEMISTRY OF SOLID STATE
V. 20, № 4 (2019) p. 376-383

DOI: 10.15330/pcss.20.4.376-383

Vasyl Stefanyk Precarpathian National University

ФІЗИКА І ХІМІЯ ТВЕРДОГО ТІЛА
Т. 20, № 4 (2019) С. 376-383

UDK 546.882 ISSN 1729-4428

M. Konyk[1], L. Romaka[1], Yu. Stadnyk[1], V.V. Romaka[2], R. Serkiz[3], A. Horyn[1]

Er-Cr-Ge Ternary System

[1]*Ivan Franko L’viv National University, L’viv, Ukraine, mariya.konyk@lnu.edu.ua*
[2]*Lviv Polytechnic National University, Lviv, Ukraine, vromaka@gmail.com*
[3]*Scientific-technical and Educational Centre of low Temperature Studies, Ivan Franko National University of Lviv, Lviv, Ukraine, rserkiz@gmail.com*

The isothermal section of the phase diagram of the Er–Cr–Ge ternary system was constructed at 1070 K over the whole concentration range using X-ray diffractometry, metallography and electron microprobe (EPM) analysis. The interaction between the elements in the Er−Cr−Ge system results in the formation of two ternary compounds: ErCr$_6$Ge$_6$ (MgFe$_6$Ge$_6$-type, space group $P6/mmm$, Pearson symbol $hP13$; a = 5.15149(3), c = 8.26250(7) Å; R_{Bragg} = 0.0493, R_F = 0.0574) and ErCr$_{1-x}$Ge$_2$ (CeNiSi$_2$-type, space group $Cmcm$, Pearson symbol $oS16$, a = 4.10271(5), b = 15.66525(17), c = 3.99017(4) Å; R_{Bragg} = 0.0473, R_F = 0.0433) at investigated temperature. For the ErCr$_{1-x}$Ge$_2$ compound, the homogeneity region was determined (ErCr$_{0.28-0.38}$Ge$_2$; a = 4.10271(5)-4.1418(9), b = 15.6652(1)-15.7581(4), c = 3.99017(4)-3.9291(1) Å).

Keywords: intermetallics; ternary system; phase equilibria; crystal structure.

Article acted received 15.08.2019; accepted for publication 15.12.2019.

Introduction

Fundamental studies of the interaction of components in the metallic systems with rare earth elements (R), transition metals (M) and *p*-elements, in particular germanium, provide important information on the formation, temperature and concentration stability of compounds to search for new materials with valuable properties.

A review of the literature data showed that the R–M–Ge systems with the participation of chromium as *d*-metal in comparison with other 3*d*-elements of the IV period (manganese, iron, cobalt, nickel, or copper) have not been sufficiently studied. An isothermal cross-section of the state diagram constructed for the Y−Cr−Ge system at 870 K showed that no ternary compounds were detected at the studied temperature [1]. In the following works the results of the crystal structure and magnetic property studies of two series of isostructural germanides were reported: RCr$_6$Ge$_6$ (R = Y, Tb−Er) [2, 3] and RCr$_x$Ge$_2$ (R = Sm, Y, Gd−Er) [4, 5]. Both series of the compounds were studied at the temperature of annealing 1 070 K. An existence of isotypic compounds YCr$_6$Ge$_6$ (MgFe$_6$Ge$_6$-type) and YCr$_{0.23}$Ge$_2$ (CeNiSi$_2$-type) was confirmed in the Y−Cr−Ge system at 1 070 K and their crystal structure was refined by X-ray powder diffraction method [6].

In this paper, we present the results of experimental investigation of the Er–Cr–Ge (1070 K) ternary system and an analysis of an influence of *d*-element on the component interaction in the R–M–Ge systems.

I. Experimental details

The alloys were prepared by a direct twofold arc melting of the constituent elements (erbium, purity of 99.9 wt.%; chromium, purity of 99.99 wt.% and germanium, purity of 99.999 wt.%) under protected argon atmosphere on a water-cooled copper crucible. For better homogenization the samples were melted twice. The weight losses of the initial total mass after arc-melting were lower than 1 wt. %. The pieces of the as-cast buttons were homogenized for one month at 1070 K in evacuated silica tubes and then water quenched. Phase analysis was performed using X-ray powder diffractions of the synthesized samples (DRON-4.0, Fe K_α radiation).

Table 1

Crystallographic characteristic of the binary phases in the Er−Ge and Cr−Ge systems at 1070 K

Phase	Space group	Structure type	Lattice parameters, Å			Reference
			a	*b*	*c*	
$ErGe_{2.83}$	*Cmcm*	$DyGe_3$	3.997	2.0605	3.887	[11]
Er_2Ge_5	*Pmmn*	Er_2Ge_5	3.872	3.993	18.125	[11]
			3.879(4)	4.005(4)	18.128(5)	this work
$ErGe_{1.83}$	*Cmcm*	$DyGe_{1.85}$	4.068	2.957	3.900	[12]
$ErGe_{1.5}$	*P6/mmm*	AlB_2	3.89		4.09	[14]
			3.886(2)		4.088(3)	this work
Er_3Ge_4	*Cmcm*	Er_3Ge_4	4.005	10.542	14.137	[13]
			4.005(3)	10.541(5)	14.134(4)	this work
ErGe	*Cmcm*	CrB	4.2199	10.581	3.906	[17]
			4.220(2)	10.581(4)	3.896(3)	this work
$Er_{11}Ge_{10}$	*I4/mmm*	$Ho_{11}Ge_{10}$	10.76		16.09	[16]
			10.763(3)		16.089(5)	this work
Er_5Ge_4	*Pnma*	Sm_5Ge_4	7.54	14.49	7.57	[15]
			7.549(3)	14.496(6)	7.576(4)	this work
Er_5Ge_3	$P6_3/mcm$	Mn_5Si_3	8.35		6.27	[15]
			8.317(3)		6.297(3)	this work
$Cr_{11}Ge_{19}$	$P\text{-}4n2$	$Mn_{11}Si_{19}$	5.79		51.87	[18]
CrGe	$P2_13$	FeSi	4.797			[20]
			4.796(3)			this work
$Cr_{11}Ge_8$	*Pnam*	$Cr_{11}Ge_8$	13.15	4.94	15.75	[19]
			13.079(5)	4.954(4)	15.721(5)	this work
Cr_3Ge	$Pm\text{-}3n$	Cr_3Si	4.631			[18]
			4.6303(1)			this work

The observed diffraction intensities were compared with reference powder patterns of the pure elements, binary and known ternary phases. The chemical and phase compositions of the obtained samples were examined by Scanning Electron Microscopy (SEM) using REMMA-102-02 scanning microscope. Quantitative electron probe microanalysis (EPMA) of the samples was carried out by using an energy-dispersive X-ray analyzer with the pure elements as standards (an acceleration voltage was 20 kV; *K*- and *L*-lines were used). The data for the crystal structure refinements were collected at room temperature using STOE STADI P diffractometer ($CuK_{\alpha1}$ radiation). Calculations of the crystallographic parameters and theoretical diffraction patterns were performed using WinCSD program package [7]. Rietveld refinement was performed using the Fullprof suite program package [8].

II. Results and discussion

2.1. Phase equilibria in the Er-Cr-Ge ternary system.

The binary boundary Er−Ge, Er−Cr and Cr−Ge systems which limit the studied Er-Cr-Ge system, have been investigated earlier and their phase diagrams are well known in the literature [9, 10]. In the Cr–Ge and Er–Ge binary systems, the existence of 4 and 9 binary compounds, respectively, were confirmed under used in our work conditions: $Cr_{11}Ge_{19}$, CrGe, $Cr_{11}Ge_8$, Cr_3Ge, $ErGe_{2.83}$, Er_2Ge_5, $ErGe_{1.83}$, $ErGe_{1.5}$, Er_3Ge_4, ErGe, $Er_{11}Ge_{10}$, Er_5Ge_4, and Er_5Ge_3. Crystallographic characteristics of the Er-Ge and Cr-Ge binary compounds are listed in Table 1.

The Cr_5Ge_3 binary compound (W_5Si_3-type) was not identified at the temperature of annealing. According to the X-ray phase analysis, the sample of the corresponding composition contained two binary phases in equilibrium: Cr_3Ge and $Cr_{11}Ge_8$. According to the literature, the Cr_5Ge_3 phase is stable only at elevated temperatures; formed by peritectic reaction at 1262ºC and decomposed eutectoid at 996ºC. Below this temperature, Cr_3Ge is in equilibrium with $Cr_{11}Ge_8$ [21].

The phase equilibria in the Er–Cr–Ge system have been established at 1070 K using the X-ray and metallographic analyses of the examined 14 binary and 33 ternary alloys. The isothermal section of the Er–Cr–Ge ternary system at corresponding temperature is illustrated in Fig. 1. The phase compositions of the selected alloys are presented in Table 2. The electron

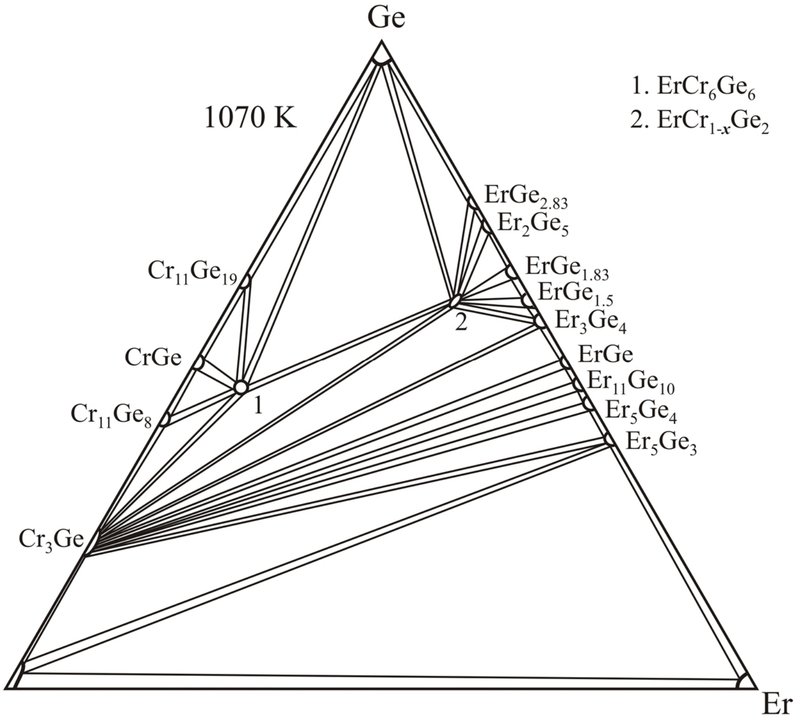

Fig. 1. Isothermal sections of the Er−Cr−Ge phase diagram at 1070 K.

Table 2

Phase composition of the selected Er−Cr−Ge alloys according to EPMA data

Phase/Component content	Er, ат.%	Cr, ат.%	Ge, ат.%
$Er_{10}Cr_{60}Ge_{30}$			
Cr_3Ge		75.34	24.66
Er_3Ge_4	43.18		56.82
$Er_{20}Cr_{20}Ge_{60}$			
$ErCr_6Ge_6$	8.74	45.52	45.74
$ErCr_{1-x}Ge_2$	31.75	6.45	51.80
(Ge)			99.96
$Er_{28}Cr_9Ge_{63}$			
$ErCr_{1-x}Ge_2$	30.28	9.12	60.60
$ErGe_{2,83}$	28.30		71.70
(Ge)			99.96
$Er_{50}Cr_{25}Ge_{25}$			
Er_5Ge_3	62.50		37.50
(Cr)		99.98	
(Er)			99.98
$Er_{50}Cr_{13}Ge_{37}$			
Er_5Ge_4	55.67		44.33
Er_5Ge_3	62.50		37.50
Cr_3Ge		72.57	27.43
$Er_{14}Cr_{44}Ge_{42}$			
$ErCr_6Ge_6$	8.91	45.23	45.86
$ErCr_{1-x}Ge_2$	29.98	11.84	58.18
Cr_3Ge		72.57	27.43

microphotographs of the some alloys are shown in Fig. 2.

No binary phases were observed in the Er−Cr system at investigated temperature [10]. The corresponding ternary samples in the region Er-Er_5Ge_3-Cr contain three phases in equilibrium – Er_5Ge_3, Er, and Cr. The solubility of the third component in the Cr−Ge and Er−Ge binaries

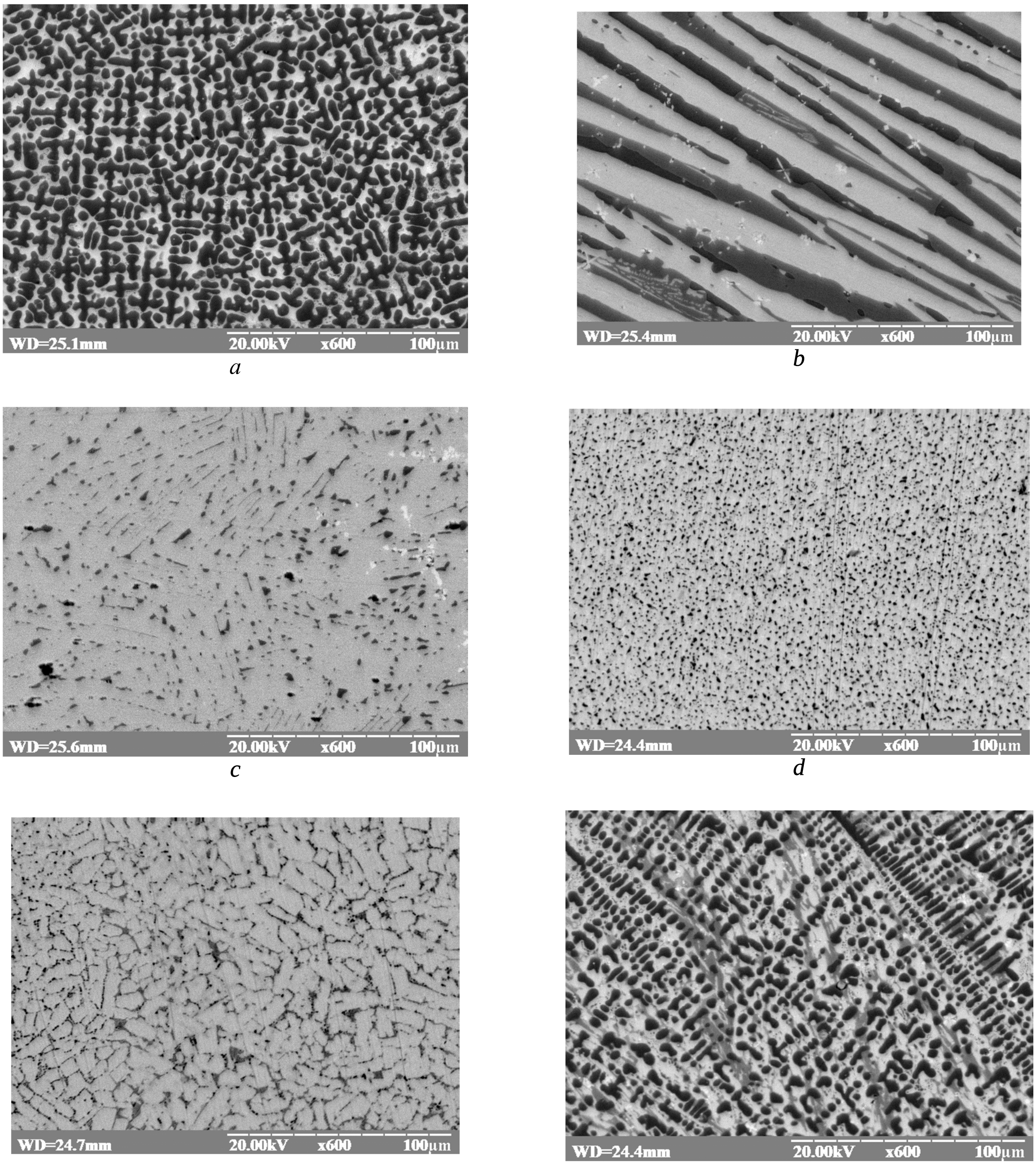

a *b*

c *d*

e *f*

Fig. 2. Electron microphotographs of the Er−Cr−Ge alloys: a) $Er_{10}Cr_{60}Ge_{30}$ – Cr_3Ge (dark phase); Er_3Ge_4 (light phase); b) $Er_{20}Cr_{20}Ge_{60}$ – $ErCr_6Ge_6$ (grey phase); $ErCr_{1-x}Ge_2$ (light grey phase); (Ge) (dark phase); c) $Er_{28}Cr_9Ge_{63}$ – $ErCr_{1-x}Ge_2$ (grey phase); $ErGe_{2,83}$ (light phase); (Ge) (dark phase); d) $Er_{50}Cr_{25}Ge_{25}$ – Er_5Ge_3 (grey phase); (Cr) (light phase); (Er) (dark phase); e) $Er_{50}Cr_{13}Ge_{37}$ – Er_5Ge_4 (grey phase); Er_5Ge_3 (light phase); Cr_3Ge (dark phase); f) $Er_{14}Cr_{44}Ge_{42}$ – $ErCr_6Ge_6$ (grey phase); $ErCr_{1-x}Ge_2$ (light phase); Cr_3Ge (dark phase).

is less than 1-2 at. % under our conditions.

2.2. Crystal structure.

According to the performed X-ray phase analysis, two ternary compounds are formed in the Er–Cr–Ge system at 1070 K. The crystal structure refinements of the ternary compounds were performed using powder diffraction data of the $Er_{10}Cr_{45}Ge_{45}$ and $Er_{30.3}Cr_{9.1}Ge_{60.6}$ samples (Figs. 3, 4). The experimental conditions of the structure refinements and the results of the structure calculation are given in Table 3, final atomic coordinates, site occupancies, and isotropic displacement parameters are presented in Table. 4.

As reported above, the authors of Ref. [1] did not establish the existence of the YCr_6Ge_6 germanide during the study of the Y−Cr−Ge system at 870 K. Further investigation of the Y−Cr−Ge system at 1070 K [6]

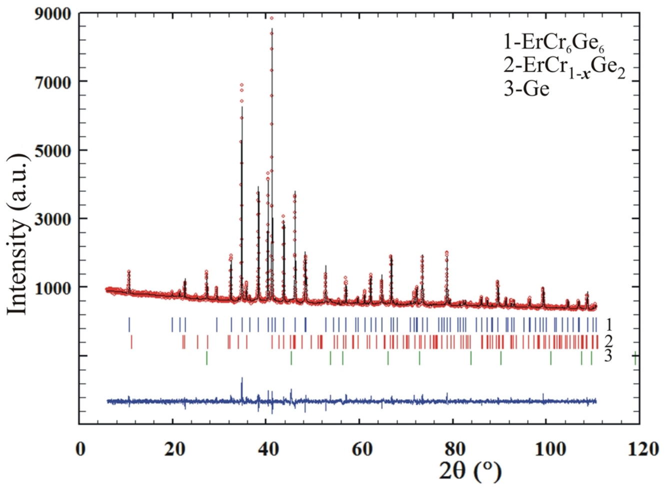

Fig. 3. The observed, calculated and difference X-ray patterns of the $Er_{10}Cr_{45}Ge_{45}$ alloy.

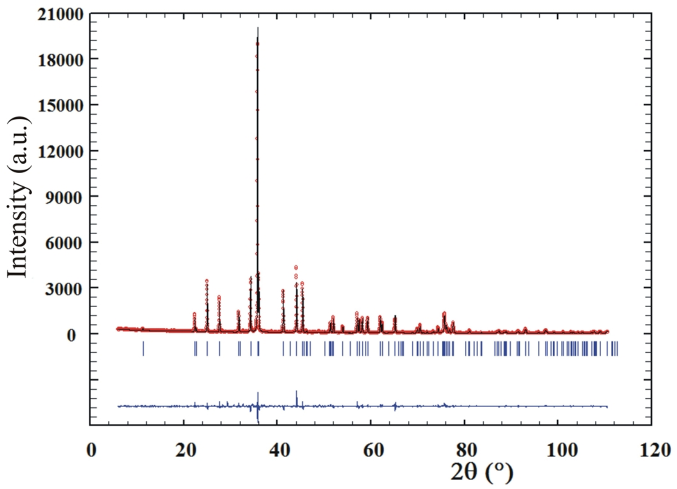

Fig. 4. The observed, calculated and difference X-ray patterns of the $ErCr_{0.28}Ge_2$ phase

Table 3

Experimental details and crystallographic data for $ErCr_6Ge_6$ and $ErCr_{0.28}Ge_2$

Alloy composition	$Er_{10}Cr_{45}Ge_{45}$	$Er_{30,3}Cr_{9,1}Ge_{60,6}$
Refined composition	$ErCr_6Ge_6$	$ErCr_{0,28(1)}Ge_2$
Overall composition from EPMA data	$Er_{8.74}Cr_{45.52}Ge_{45.74}$	$Er_{30.28}Cr_{9.12}Ge_{60.60}$
Structure type	$MgFe_6Ge_6$	$CeNiSi_2$
Pearson symbol	*hP*13	*oS*16
Space group; Z	*P6/mmm* (No. 191); 2	*Cmcm* (No. 63) 4
Unit-cell parameters: *a, b, c,* Å	5.15149(3); 8.26250(7)	4.10271(5); 15.6652(1); 3.99017(4)
Cell volume V, $Å^3$	189.892	256.448
Calculated density D_x, g/cm^3	8.000	8.474
Diffractometer	STOE STADI P (transmission mode, curved Ge(111) monochromator on primary beam)	
Radiation, wavelength λ (Å)	Cu K_α, 1,54056	
Angular range for data collection / increment (°$2q$)	6.000≤$2q$≤110.6255 / 0.015	
Linear PSD step (°$2q$) /time (sec/step)	0.480 / 220	0.480 / 250
Half width parameters: *U, V, W, η*	0.003(1), -0.006(2), 0.006(2), -0.33(1)	0.081(4), -0.028(4), 0.0152(8), 0.428(8)
Asymmetry parameters	0.0076(0), 0.0154(0)	0.043(3), 0.014(1)
Reliability factors: R_{Bragg}; R_F	0.0493; 0.0574	0.0473; 0.0433
Content of $ErCr_6Ge_6$ / $ErCr_{0,28}Ge_2$ / Ge phases (wt. %)	93.48 / 2.55 / 3.97	

Table 4

Atomic coordinates, site occupancies and isotropic displacement parameters for $ErCr_6Ge_6$ and $ErCr_{0.28}Ge_2$

Atom	Wyckoff position	*x*	*y*	*z*	*G*	B_{iso}, Å^2
$ErCr_6Ge_6$						
Er	1*a*	0	0	0	1	1.21(7)
Cr	6*i*	1/2	0	0.2510(2)	1	0.51(5)
Ge1	2*e*	0	0	0.3503(3)	1	1.12(7)
Ge2	2*d*	1/3	2/3	1/2	1	0.28(7)
Ge3	2*c*	1/3	2/3	0	1	0.11(7)
$ErCr_{0.28}Ge_2$						
Er	4*c*	0	0.3969(8)	1/4	1	0.24(4)
Cr	4*c*	0	0.2034(7)	1/4	0.28(1)	0.51(0)
Ge1	4*c*	0	0.0534(1)	1/4	1	0.56(2)
Ge2	4*c*	0	0.7518(1)	1/4	1	1.72(5)

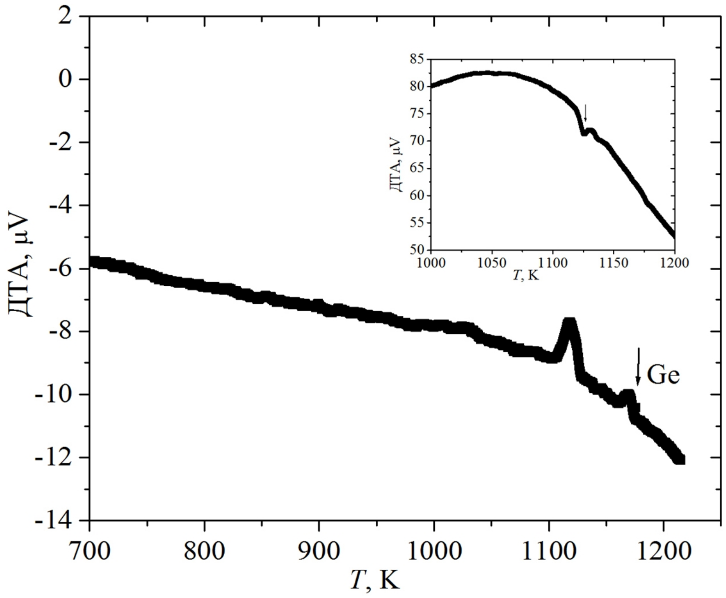

Fig. 5. DTA curve for the $ErCr_6Ge_6$ compound (crystallization and melting curve (inset).

revealed the formation of the YCr_6Ge_6 compound, and DTA indicated its existence in a rather wide temperature range up to 1120 K. As reported in Refs. [2, 3] isotypic RCr_6Ge_6 germanides where R = Tb-Er, were also obtained at annealing temperature 1070 K. To check the temperature interval of stability of the $ErCr_6Ge_6$ compound, a differential thermal analysis (synchronous LINSEIS STA PT 1600 thermoanalyzer) was performed, according to which the $ErCr_6Ge_6$ compound exists up to temperature of 1126 K, above which it decomposes (Fig. 5).

Conclusions

An experimental study of the interaction of components in the Er–Cr–Ge ternary system at 1070 K confirmed the formation of two ternary germanides, $ErCr_6Ge_6$ and $ErCr_{1-x}Ge_2$, which were reported earlier. Compound $ErCr_6Ge_6$ is characterized by stoichiometric composition, while for $ErCr_{1-x}Ge_2$ compound with the $CeNiSi_2$ structure type the small homogeneity range was established. $ErCr_{0.30}Ge_2$ composition reported in Ref. [4] is included into the homogeneity region of the $ErCr_{1-x}Ge_2$ compound which was established in our work. The investigated Er–Cr–Ge system by the nature of phase equilibria, the number of ternary compounds and their crystal structure is similar to the studied Y−Cr−Ge (1070 K) system [6]. The similar interaction of components can be predicted for the systems with other rare earth metals, including gadolinium, terbium, dysprosium, for which RCr_6Ge_6 and $RCr_{1-x}Ge_2$ compounds are known. The formation of isostructural compounds RCr_6Ge_6 and $RCr_{1-x}Ge_2$ also with Tm, Yb, Lu is not excluded.

In contrast to the RCr_6Ge_6 and $RCr_{1-x}Ge_2$ germanides formed with rare earth elements of the Yttrium group, an isostructural series of $RCrGe_3$ compounds (R = La-Nd, Sm, $BaNiO_3$-type, space group $P6_3/mmc$) is realized for the rare earths of cerium group [31]. Similar compounds with the perovskite-type structure are also formed with the vanadium $RVGe_3$ (R = La-Nd, Sm) [32]. It worth to note, that this structure type is not peculiar to the germanides with other transition metals. Additionally, $R_{117}Cr_{52}Ge_{112}$ compounds with a cubic $Tb_{117}Fe_{52}Ge_{112}$ structure type were found for Nd and Sm [33, 34].

Ternary $RM_{1-x}Ge_2$ compounds with the $CeNiSi_2$ structure type are most often realized in the R−M−Ge systems, as indicated by the isostructural series $RCr_{1-x}Ge_2$ (R = Y, Sm, Gd-Er), $RMn_{1-x}Ge_2$ (R = Y, Nd, Sm, Gd-Tm, Lu), $RFe_{1-x}Ge_2$ (R = Y, La-Sm, Gd-Lu), $RCo_{1-x}Ge_2$ (R = Y, La-Sm, Gd-Lu), $RNi_{1-x}Ge_2$ (R = Y, La-Lu), $RCu_{1-x}Ge_2$ (R = La-Sm, Gd-Tm, Lu) [25-28].

Comparison of the studied Er–Cr–Ge system with other Er–M–Ge systems where M = Mn, Fe, Co, Ni, or Cu [22–24], indicates that the character of phase equilibria, the number of ternary compounds and the type of their crystal structure are depend on the M-component. Passing from chromium to the metals of iron group indicates the complicated character of the component interaction in the Er–M–Ge systems with increasing the number of the ternary compounds. In the Er–Mn–Ge (870 K) system, 4 ternary compounds were formed, and in the Er–{Fe, Co, Ni}–Ge (1070 K) systems, 8, 16, 14 ternary germanides are realized at annealing temperatures, respectively. Passing to the copper leads to a decrease in the number of ternary compounds. Subsequently only six ternary compounds were observed in the Er−Cu−Ge system at 870 K [23]. Similar tendency is observed for other R–M–Ge systems. For example, for the yttrium, the interaction of the components in the Y−{V, Cr, Mn, Fe, Ni}−Ge systems was investigated over the whole concentration range [6, 24, 29, 30]. In the Y–{Co, Cu}–Ge systems some intermetallics as representatives of isostructural series were studied only [24]. When V is replaced by Cr, Mn, Fe, Co, and Ni, the number of the ternary germanides increases significantly 1 → 2 → 4 → 5 → 7 → 10, and decreases to six when passing to the Y–Cu–Ge system.

Acknowledgement

We would like to acknowledge financial support of the Ministry of Education and Science of Ukraine under Grant No 0118U003609.

Konyk M. **-** Ph.D., Senior Research;
Romaka L. **-** Ph.D., Senior Scientist;
Stadnyk Yu. **-** Ph.D., Senior Scientist;
Romaka V. **-** D.Sc., Assoc. Professor;
Serkiz R. **-** Senior Research;
Horyn A. **-** Ph.D., Senior Research.

[1] O.I. Bodak, E.I. Gladyshevsky, Ternary systems containing rare earth metals (Vyshcha shkola, Lviv, 1985).
[2] J.H.V.J. Brabers, K.H.J. Buschow, F.R. de Boer, J. Alloys Compd. 77, 205 (1994). (DOI: 10.1016/0925-8388(94)90769-2).
[3] P. Schobinger-Papamantelljsa, J. Rodriguez-Carvajalb, K.H.J. Buschow, J. Alloys Compd. 92, 256 (1997). (doi.org/S0925-8388(96)03109-X).
[4] H. Bie, A. Tkachuk, A.Mar, J. Solid State Chemistry 182(1), 122 (2009). (doi.org/10.1016/j.jssc.2008.10.013).
[5] A. Gil, D. Kaczorowski, B. Penc, A. Hoser, A. Szytula, J. Solid State Chem. 227, 184(2) (2011). (doi.org/10.1016/j.jssc.2010.10.026/).
[6] M. Konyk, L. Romaka, L. Orovčik, V.V. Romaka, Yu. Stadnyk, Visnyk Lviv Univ. Ser. Chem. Вісн. 38, 60(1) (2019). (doi.org/10.30970/vch.6001.038).
[7] L. Akselrud, Yu. Grin. WinCSD: software package for crystallographic calculations (Version 4). J. Appl. Cryst. 47, 803 (2014). (doi.org/10.1107/S1600576714001058).
[8] T. Roisnel, J. Rodriguez-Carvajal, WinPLOTR: a Windows tool for powder diffraction patterns analysis. Mater. Sci. Forum. 378, 118 (2001).
[9] T.B. Massalski, in: Binary Alloy Phase Diagrams (ASM, Metals Park, Ohio, 1990).
[10] Okamoto H. Desk Handbook: Phase Diagrams for Binary Alloys (Materials Park (OH), American Society for Metals, 2000).
[11] G. Venturini, I. Ijjaali, B. Malaman, J. Alloys Compd. 288(1-2), 183 (1999). (doi.org/10.1016/S0925-8388(99)00088-2).
[12] O. Oleksyn, P. Schobinger-Papamantellos, C. Ritter, C.H. Groot, K.H.J. Buschow, J. Alloys Compd. 252(1-2), 53 (1997). (doi.org/10.1016/S0925-8388(96)02714-4).
[13] O.Ya. Oleksyn, O.I. Bodak, J. Alloys Compd., 210(1-2), 19 (1994). (doi.org/10.1016/0925-8388(94)90108-2).
[14] G. Venturini, I. Ijjaali, B. Malaman, J. Alloys Compd. 284(1-2), 262 (1999). (doi.org/10.1016/S0925-8388(98)00958-X).
[15] G.S. Smith, A.G. Tharp, Q. Johnson, J. Acta Crystallogr. 22, 940 (1967). (doi.org/10.1107/S0363110X67001902).
[16] V.N. Eremenko, I.M. Obuschenko, Sov. Non-Ferrous Met. Res. 216, 9 (1981).
[17] P. Schobinger-Papamantellos, K.H.J. Buschow, J. Less Common Met. 111(1-2), 117 (1985). (doi.org/10.1016/0022-5088(85)90177-8).

[18] M. Kolenda, J. Stoch, A. Szytula, J. Magn. Magn. Mater. 20(1), 99 (1980). (doi.org/10.1016/0304-8853(80)90532-6)

[19] B. Rawal, K.P. Gupta, J. Less Common Met. 27(1), 65 (1972). (doi.org/10.1016/0022-5088(72)90105-1).

[20] T. Sato, E. Ohta, M. Sakata, J. Magn. Magn. Mater. 61(1-2), 205 (1986). (doi.org/10.1016/0304-8853(86)90085-5).

[21] I. Jandl, K.W. Richter, J. Alloys Compd. 500(1), L6 (2010). (DOI: 10.1016/j.jallcom.2010.03.200).

[22] M.B. Konyk, L.P. Romaka, V.V. Romaka, R.Ya. Serkiz, Phys. Chem. Solid State 13(4), 956, (2012).

[23] M. Konyk, A. Horyn, R. Serkiz, Visnyk Lviv. Univ. Ser. Chem. 42, 53 (2012).

[24] P.S. Salamakha, O.L. Sologub, O.I. Bodak, In: Gschneidner K. A. et al (Eds.), Ternary rare-earth germanium systems, Handbook on the Physics and Chemistry of Rare Earths, Vol 27 (The Netherlands, Amsterdam, 1999).

[25] V.K. Pecharsky, O.Ya. Mruz, M.B. Konyk, P.S. Salamakha, P.K. Starodub, M.F. Fedyna, O.I. Bodak, J. Struct. Chem. 30(5), 96 (1989).

[26] M. Francois, G. Venturini, B. Malaman, B. Roques, J. Less-Common Met. 160(2), 197 (1990). (doi.org/10.1016/0022-5088(90)90381-S).

[27] R. Duraj, M. Konyk, J. Przewoznik, L. Romaka, A. Szytula, Solid State Sci. 25, 11 (2013). (dx.doi.org/10.1016/j.solidstatesciences.2013.07.019)

[28] L. Romaka, M. Konyk, Yu. Stadnyk, V.V. Romaka, R. Serkiz, Phys. Chem. Solid State 20(1), 69, (2019). (DOI: 10.15330/pcss.20.1.69-76).

[29] M. Konyk, L. Romaka, A. Horyn, N. German, R. Serkiz, Visnyk Lviv Univ. Ser. Chem. 56, 25 (2015).

[30] M. Konyk, L. Romaka, Yu. Stadnyk, V.V. Romaka, R. Serkiz, Visnyk Lviv Univ. Ser. Chem. 59(1), 11 (2018). (doi.org/10/30970/vch.5901.011).

[31] H. Bie, O.Ya. Zelinska, A.V. Tkachuk, A. Mar, J. Mater. Chem. 19(18), 4613 (2007). (doi.org/10.1021/cm0727+).

[32] H. Bie, A. Mar, J. Mater. Chem., 19, 6225 (2009) (doi.org/10.1039/B908781H).

[33] A.V. Morozkin, Y.D. Seropegin, V. K. Portnoy, I.A. Sviridov, A.V. Leonov, Mater. Res. Bull. 33(6), 903 (1998). (doi.org/10.1016/S0025-5408(98)00051-8).

[34] P.S. Salamakha, Yu.M. Prots, O.L. Sologub, O.I. Bodak, J. Alloys Compd. 51, 215 (1994). (doi.org/10.1016/0925-8388(94)908817-6).

М. Коник[1], Л. Ромака[1], Ю. Стадник[1], В.В. Ромака[2], Р. Серкіз[3], А. Горинь[1]

Потрійна система Er-Cr-Ge

[1]*Львівський національний університет ім. І.Франка, Львів, Україна, mariya.konyk@lnu.edu.ua,*
[2]*Національний університет “Львівська політехніка”, Львів, Україна, vromaka@gmail.com*
[3]*Науково-технічний і навчальний центр низькотемпературних досліджень, Львівський національний університет імені І. Франка, Львів, Україна, e-mail: rserkiz@gmail.com*

Ізотермічний переріз діаграми стану потрійної системи Er–Cr–Ge побудований за температури 1070 K в повному концентраційному інтервалі методами рентгенофазового, рентгеноструктурного і мікроструктурного аналізів. Взаємодія компонентів у системі Er–Cr–Ge за температури дослідження характеризується утворенням двох тернарних сполук $ErCr_6Ge_6$ (структурний тип $MgFe_6Ge_6$, просторова група *P*6/*mmm*, символ Пірсона *hP*13; *a* = 5,15149(3), *c* = 8,26250(7) Å; R_{Bragg} = 0,0493, R_F = 0,0574) і $ErCr_{1-x}Ge_2$ (структурний тип $CeNiSi_2$, просторова група *Cmcm*, символ Пірсона *oS*16, *a* = 4,10271(5), *b* = 15,6652(1), *c* = 3,99017(4) Å; R_{Bragg} = 0,0473, R_F = 0,0433). Для сполуки $ErCr_{1-x}Ge_2$ визначена область гомогенності ($ErCr_{0,28-0,38}Ge_2$; *a* = 4,10271(5)-4,1418(9), *b* = 15,6652(1)-15,7581(4), *c* = 3,99017(4)-3,9291(1) Å).

Ключові слова: інтерметаліди, потрійна система, фазові рівноваги, кристалічна структура.